

## Effects of Complex System Topology on the Bak-Sneppen Evolution Model

L. Guo\* and X. Cai

*Complexity Science Center and Institute of Particle Physics, Huazhong (Central China) Normal University, Wuhan, 430079, China.*

Received 4 May 2009; Accepted (in revised version) 3 June 2009

Communicated by Dietrich Stauffer

Available online 1 September 2009

---

**Abstract.** In this paper, we investigate by numerical simulations the Bak-Sneppen model (BSM) for biological evolution on scale-free networks (SFNs) with various degree exponents  $\gamma$ . We find that the punctuated equilibrium is rather robust with respect to the network topology. Furthermore, we analyze the evolution of the critical average fitness  $\langle f \rangle_*$  and the exponent  $\tau$  of  $\langle f \rangle_0$  avalanche as a function of  $\alpha$  (i.e., the degree exponent  $\gamma$ ). Our observations indicate the dependence of evolutionary dynamics of BSM on the complex biosystem topology.

**PACS:** 05.65.+b, 87.23.Kg, 89.75.-k

**Key words:** Complex system topology, Bak-Sneppen model, punctuated equilibrium, the average fitness.

---

### 1 Introduction

The Bak-Sneppen model (BSM) [1], which was proposed by Bak and Sneppen in 1993, can generate the punctuated equilibrium behavior observed in the evolution of many species. In the BSM, random numbers  $f_i$ , drawn from a uniform distribution between 0 and 1,  $p(f)$ , are assigned to each species located on an  $n$ -dimensional lattice with periodic boundary conditions. At each time step, the extinct species, i.e., the species with the smallest random number, and all its nearest neighboring species, are assigned new random numbers also chosen from  $p(f)$ . After a long transient process the system evolves into a self-organized critical state which is statistically stationary, where the density of fitness values in the system is uniform above  $f_c$  (the self-organized threshold) and vanishes for  $f < f_c$ , and the avalanches of mutations occur on all scales.

---

\*Corresponding author. *Email addresses:* longkuo0314@gmail.com (L. Guo), xcai@mail.ccnu.edu.cn (X. Cai)

Despite the fact that it is an oversimplification of the evolution of real species, the BSM shows some common interesting features observed by paleontologists, such as the punctuated equilibrium, power-law probability distributions of lifetimes of species and sizes of extinction events [2]. Since the BSM was introduced, the model has been paid much attention. For instance, Li and Cai [2, 3] studied different hierarchy of avalanches, exact equations and scaling relations for  $\langle f \rangle_0$  avalanches in the BSM. On the other hand, many real biological networks, such as the food webs [4, 5], the metabolic networks [6, 7] and the protein networks [8, 9], share some universal characteristics such as the small-world effect and the power-law degree distribution  $p(k) \sim k^{-\gamma}$ . These features may affect the dynamics of the networks on which the species are placed. Hence, it is important to study the effects of complex biosystems topology on the evolutionary dynamics of BSM. Recently, the BSM has been studied on random networks (RNs) [10], small-world networks (SWNs) [11] and scale-free networks (SFNs) [12, 13]. Moreno and Vazquez studied the avalanche size distribution and the activity time behavior at nodes with different connectivity of BSM only on a SFN with  $\gamma = 3$  [12]. Lee and Kim studied the dependence of the critical fitness  $f_c$  and the avalanche size distribution  $P(S)$  on the connectivity property of SFN [13], from the viewpoint of microscopic. Here, we focus on the dependence of the evolutionary dynamics of BSM on the complex system topology, especially the exponent of the connectivity distribution, from the viewpoint of macroscopic.

In order to do this, we study the evolutionary dynamics of BSM on SFNs, which is generated by using the static model [15] instead of the preferential attachment growth algorithm [16], with various degree exponent  $\gamma \in (2, \infty)$ . Generically, the system reaches a steady state where the average fitness  $\langle f \rangle$  approaches a critical value  $\langle f \rangle_*$  and all the  $\langle f \rangle$ s are smaller than the critical average fitness  $\langle f \rangle_*$  as time  $t \rightarrow \infty$ . And the  $\langle f \rangle_*$  decreases with the tunable parameter  $\alpha$ , which is related to the degree exponent  $\gamma$  via  $\gamma = (1 + \alpha) / \alpha$ , increasing. On the other hand, SFNs with the degree exponent  $2 < \gamma \leq 3$  are physically different from those with  $\gamma > 3$  [14]. Furthermore, we focus on the evolution of  $\langle f \rangle_*$  and the exponent  $\tau$  of the  $\langle f \rangle_0$  avalanche size distribution  $P(S) \sim S^{-\tau}$  as a function of the parameter  $\alpha$ , i.e., the degree exponent  $\gamma$ . We find that the complex network structure plays a crucial role in the evolutionary dynamics of BSM. Furthermore, we analyze  $\langle f \rangle_*$  as a function of  $\alpha$  on SFNs with various system sizes  $N$ , and find that the BSM on SFNs with  $2 < \gamma \leq 3$  self-organizes into a stationary state where the critical average fitness  $\langle f \rangle_* \rightarrow 0.5$  for  $N \rightarrow \infty$ , just as  $f_c \rightarrow 0$  for  $N \rightarrow \infty$  found in [12, 13]. Finally, we classify the SFNs into three different categories: random for  $\gamma > 4.3$ , linear for  $3 < \gamma < 4.3$  and physical for  $2 < \gamma \leq 3$ , from the viewpoint of dynamics.

## 2 Model

Many real biological systems can be well mapped to complex networks, which are sets of nodes  $i = 1, 2, \dots, N$ , connected by a number of  $l = 1, 2, \dots, L$  edges. The network is represented by its adjacency matrix  $A$ , where  $A_{ij} = 1$ , if an edge connects nodes  $i$  and  $j$

and  $A_{ij} = 0$ , otherwise. We do not consider self-connections or multiple edges.

To construct SFNs with various degree exponents  $\gamma$ , we employ the standard method proposed in the static model [15] instead of the preferential attachment growth algorithm [16]. We start with  $N$  nodes, each of which is indexed by an integer  $i (i = 1, 2, \dots, N)$  and assigned a weight  $p_i = i^{-\alpha}$ . Here  $\alpha$  is a control parameter in  $[0, 1)$ . Next, we select two different nodes  $(i, j)$  with probabilities equal to the normalized weights,  $p_i / \sum_k p_k$  and  $p_j / \sum_k p_k$ , respectively, and add an edge between them unless one exists already. This process is repeated until  $mN$  edges are made in the system. In our present work, we use  $N = 1000$  and  $m = 2$ . Numerical simulations indicate that this network evolves into a scale-invariant state with the probability that a node has  $k$  edges following a power law with the exponent  $\gamma = (1 + \alpha) / \alpha$ . Thus, adjusting the parameter  $\alpha$  in  $[0, 1)$ , we can obtain various values of the exponent  $\gamma$  in the range of  $(2, \infty)$ .

### 3 Results

We simulate the dynamics of BSM on SFNs of size  $N = 1000$  with various parameter  $\alpha \in [0, 1)$ . The initial fitness  $f$  of species is randomly chosen from a uniform distribution between 0 and 1,  $p(f)$ . All the results have been averaged over at least 20 realizations, with each running lasting for at least  $10^7$  updating steps.

The average fitness [3], denoted by  $\langle f \rangle$ , is a global one of the ecosystem and can be expected to involve some general information about the whole system. It may represent the average population or living capability of the whole species system. A larger  $\langle f \rangle$  shows that the average population is large or the average living capability is great, and vice versa.  $\langle f \rangle$  is defined as

$$\langle f \rangle = \frac{1}{N} \sum_{i=1}^N f_i, \quad (3.1)$$

where  $f_i$  is the fitness of the  $i$ -th species of a system consisting of  $N$  species. At each time step of the evolution, apart from the fitnesses of the globally extremal site (i.e., the site with the smallest fitness) and its  $k$  nearest neighboring sites, the signal  $\langle f \rangle$  is also tracked. Initially,  $\langle f \rangle$  tends to increase stepwisely (see the Inset in Fig. 1) with larger fluctuation than that on D-dimensional lattices [3], probably caused by the heterogeneous property of SFNs. However, as the evolution continues further,  $\langle f \rangle$  approaches a critical value  $\langle f \rangle_*$  and all the  $\langle f \rangle$ s are smaller than the critical average fitness  $\langle f \rangle_*$  as time  $t \rightarrow \infty$ . The plots of  $\langle f \rangle$  versus time step  $t$  show that the increasing extremal value of  $\langle f \rangle$  follows a Devil's staircase, which indicates that the punctuated equilibrium emerges. Further, we study the gap of the punctuated equilibrium, denoted by  $F(s)$ , on SFNs with various  $\alpha$ . The definition of  $F(s)$  is given as follows [3]: Initial value of  $F(s)$  is equal to  $\langle f \rangle(0)$ . After  $t$  updates, a larger  $F(t) > F(0)$  opens up. The current gap  $F(t)$  is the maximum of all  $\langle f \rangle(t')$ , for all  $0 \leq t' < t$ . For convenience, we change the current time  $t$  to the symbol  $s$  and  $F(t)$  to  $F(s)$ , since  $F(s)$  tracks the peaks in  $\langle f \rangle$  [2] that is different from the evolution of  $\langle f \rangle$  as a function of time  $t$ . In Fig. 1 we represent the evolution of  $F(s)$  as a staircase increasing

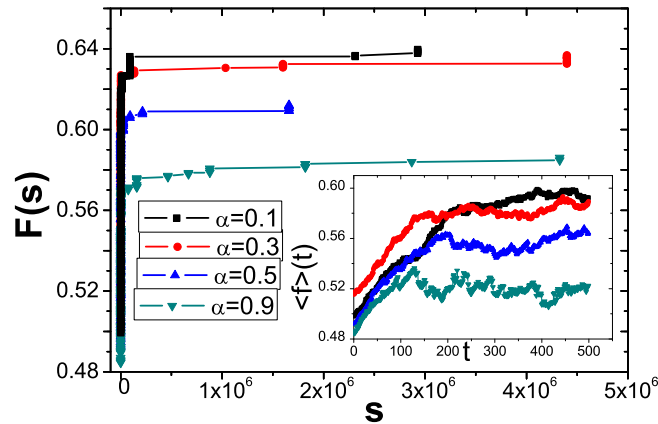


Figure 1: (color online) Punctuated equilibrium of  $\langle f \rangle$  for the evolutionary dynamics of BSM on SFNs with various degree exponent  $\gamma(=(1+\alpha)/\alpha)$ . We track the increasing extremal value of  $\langle f \rangle$ , i.e.,  $F(s)$ . Inset: the variation of  $\langle f \rangle$  versus  $t$  during a time period on the SFNs with various degree exponent  $\gamma$  ( $\alpha$ ) = 11(0.1), 4.3(0.3), 3(0.5), and 2.1(0.9), from up to down. The parameters of the static scale-free network are  $N=1000$  and  $m=2$ .

function of  $s$  during the transient on SFNs with various degree exponents  $\gamma(=(1+\alpha)/\alpha)$ . Actually, the gap is an envelope function that tracks the peaks in  $\langle f \rangle$  and finally reaches a critical average fitness  $\langle f \rangle_*$ , which had been observed on lower (1 or 2) dimensional lattices [3]. Interesting,  $\langle f \rangle_*(\alpha)$  increases with increasing  $\alpha$ . While  $\langle f \rangle_*$  is smaller than that on 1- and 2-dimensional lattices [3].

Further light can be shed on the effects of the SFN's topology on the evolutionary dynamics of the given BSM. In order to do this, we study the dependence of  $\langle f \rangle_*$  and the exponent  $\tau$  of  $f_0$  avalanche on  $\alpha$ , i.e., the exponent  $\gamma$  of the degree distribution, respectively.

As well known, the highest connectivity in SFNs increases with  $\alpha$  increasing. Namely, the larger the parameter  $\alpha$  is, the more heterogeneous the complex network is. In Fig. 2 we represent the evolution of  $\langle f \rangle_*$  as a function of  $\alpha$ , which shows the role of the heterogeneity of complex system topology in the evolutionary dynamics of BSM. We find that  $\langle f \rangle_*$  decreases with increasing  $\alpha$ , i.e., the more heterogeneous the complex system is, the smaller the  $\langle f \rangle_*$  will be. On the other hand, the  $\langle f \rangle_*$  in SFN ( $2 < \gamma < 3$ ) is smaller than that in random network ( $\alpha=0$ ) and regular lattice [3], which indicates that the homogeneous property of complex system enhances the fitness of complex system. The smallest  $\langle f \rangle_*|_{\alpha=1}$  is close to 0.5, which has a strong relationship with the complex system size  $N$ , see the inset (a) of Fig. 2. We find that  $\langle f \rangle_*$  decreases as the size  $N$  increases.

In order to show the finite-size effect of the BSM on complex system further, we represent the evolution of  $\langle f \rangle_*$  as a function of  $N$  of complex system with various  $\alpha$  in Fig. 3. We find that the more larger the complex system size  $N$  is, and the more heterogeneous the complex system is, the smaller the  $\langle f \rangle_*$  of the complex system is. In the inset of Fig. 3,

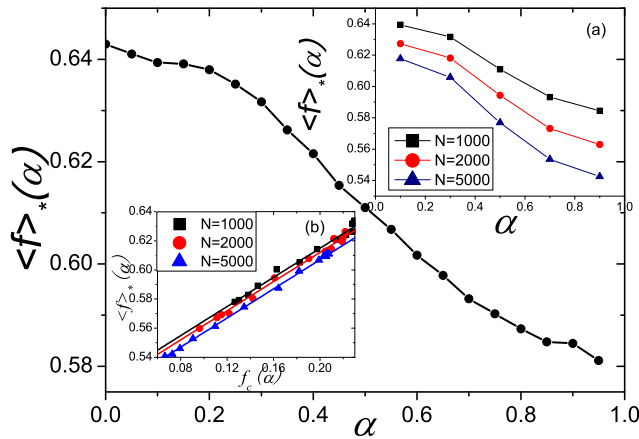


Figure 2: (color online) The evolution of  $\langle f \rangle_*$  as a function of  $\alpha$ . The network parameters are as in Fig. 1. Insets: (a) The evolution of  $\langle f \rangle_*$  as a function of  $\alpha$  on SFNs with various size  $N=1000,2000$  and  $5000$ . (b) The evolution of the critical average fitness  $\langle f \rangle_*(\alpha)$  as a function of the critical minimum fitness  $f_c(\alpha)$  on the complex networks with the size  $N=1000$  (square),  $2000$  (circle) and  $5000$  (triangle). Each dot shows the relationship between  $\langle f \rangle_*(\alpha)$  and  $f_c(\alpha)$  on the complex network with  $\alpha$ . The solid lines represent the linear fitting functions as the form of  $\langle f \rangle_*(\alpha) = (B + f_c(\alpha))/2$ , where  $B=1.029$  for  $N=1000$ ,  $B=1.024$  for  $N=2000$  and  $B=1.014$  for  $N=5000$ , from top to bottom.

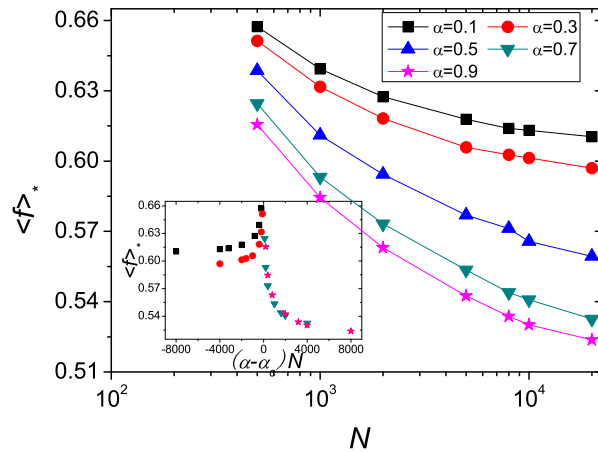


Figure 3: (color online) The evolution of  $\langle f \rangle_*$  as a function of the size  $N$  of SFNs with various parameter  $\alpha$ . The main plot shows the unscaled results, showing the  $\langle f \rangle_*$  decreases as the control parameter  $\alpha$  increases. The inset shows the scaling law  $\langle f \rangle_* = \langle f \rangle_*((\alpha - \alpha_c)N)$  with  $\alpha_c = 0.5$  for  $\alpha > \alpha_c$  (i.e.,  $2 < \gamma < 3$ ).

for  $0.5 < \alpha < 1$  ( $2 < \gamma < 3$ ), a finite size scaling analysis shows that the data can be well fitted by the formula:

$$\langle f \rangle_* = \langle f \rangle_*((\alpha - \alpha_c)N), \tag{3.2}$$

where  $\alpha_c = 0.5$  ( $\gamma = 3$ ) is the critical parameter (exponent) that divides SFNs into the physical ones and the non-physical ones. For  $0.5 < \alpha < 1$  ( $2 < \gamma < 3$ ),  $\langle f \rangle_*$  approaches to  $0.5$  as  $N$  goes to  $\infty$ ; while, for  $\alpha < 0.5$  ( $\gamma > 3$ ), the  $\langle f \rangle_*$  decreases slower than that for

$0.5 < \alpha < 1$  ( $2 < \gamma < 3$ ), and  $\langle f \rangle_*(N \rightarrow \infty) \rightarrow \text{const}$  ( $> 0.5$ ) for  $\alpha < 0.5$  ( $\gamma > 3$ ). What is more, we also study the relationship between the critical average fitness  $\langle f \rangle_*(\alpha)$  and the critical minimum fitness  $f_c(\alpha)$ , see the inset (b) in the Fig. 2. We find that the critical average fitness  $\langle f \rangle_*(\alpha)$  and the critical minimum fitness  $f_c(\alpha)$  are related by

$$\langle f \rangle_*(\alpha) = \frac{1}{2}(B + f_c(\alpha)),$$

where  $B$  is the fitting parameter. Here,  $B = 1.029$  for  $N = 1000$ ,  $B = 1.024$  for  $N = 2000$  and  $B = 1.014$  for  $N = 5000$ . The result that the parameter  $B$  is close to one shows that above the  $f_c$  the density of  $f$  values is uniform. Hence, for  $2 < \gamma < 3$ ,  $f_c \rightarrow 0$  as  $N$  goes to  $\infty$  and for  $\gamma > 3$ ,  $f_c(N \rightarrow \infty) \rightarrow \text{const}$  ( $> 0$ ), which had been shown by Lee and Kim from the viewpoint of microscopic [13].

Finally, we study the effects of SFN's topology on the  $\langle f \rangle_0$  avalanche [18], which is based on the  $f_0$  avalanche. The idea of  $f_0$  avalanche, i.e., PMB avalanches which had been proposed by Paczuski et al. [17], originated from BS avalanches. The revolutionary PMB avalanche greatly puts forward our understanding of the dynamics of the evolution model. And the  $\langle f \rangle_0$ , between 0.5 and 1, is an auxiliary parameter in defining the avalanche. Smaller avalanches merge into bigger ones as  $\langle f \rangle_0$  increases, and larger avalanches split into smaller ones as  $\langle f \rangle_0$  decreases [18]. Here, the  $\langle f \rangle_0$  avalanche is defined as follows: suppose at time step  $t_1$ ,  $\langle f \rangle(t_1)$  is greater than  $\langle f \rangle_0$ . If, at time step  $(t_1 + 1)$ ,  $\langle f \rangle(t_1 + 1)$  is less than  $\langle f \rangle_0$ , this update mechanism initiates a creation-annihilation branching process. The avalanche still continues at time step  $t'$ , if all the  $\langle f \rangle(t)$  are less than  $\langle f \rangle_0$  for  $t_1 < t \leq t' - 1$ . The avalanche stops, say, at time step  $(t_1 + S)$ , when  $\langle f \rangle(t_1 + S) > \langle f \rangle_0$ . In terms of this definition, the size of the avalanche is the number of time steps between subsequent punctuation of the barrier  $\langle f \rangle_0$  by the signal  $\langle f \rangle(t)$ . In the above example, the size of the avalanche is  $S$  [3]. This definition properly embodies the spatiotemporal features of  $\langle f \rangle_0$  avalanche on complex systems. Here, we study the property of the  $\langle f \rangle_0$  avalanche when  $\langle f \rangle_0$  is close to the critical average fitness  $\langle f \rangle_*(\alpha)$  for each network with  $\alpha$ . In order to do this, we choose  $\langle f \rangle_0$  to satisfy

$$\langle f \rangle_0(\alpha) = \langle f \rangle_*(\alpha)|_{\alpha=0.05} - 0.02 - k(N) \times (\alpha - 0.05),$$

where 0.05 is the initial condition for  $\alpha$  and  $k(N)$ s are 0.075, 0.08, 0.1 for  $N=1000, 2000$  and 5000, respectively. Here, we choose the form of the function  $\langle f \rangle_0(\alpha)$ , which guaranties that the  $\langle f \rangle_0(\alpha)$  is chosen as the critical average fitness  $\langle f \rangle_*(\alpha)$  and

$$(\langle f \rangle_*(\alpha) - \langle f \rangle_0(\alpha)) < 0.02$$

for different  $\alpha$ . In Fig. 4 we show the size distribution of  $\langle f \rangle_0$  avalanche on SFNs with size  $N = 1000$ . The probability distribution  $P(S)$  of avalanche size  $S$  on the SFNs follows the power law distribution

$$P(S) \sim S^{-\tau}, \quad (3.3)$$

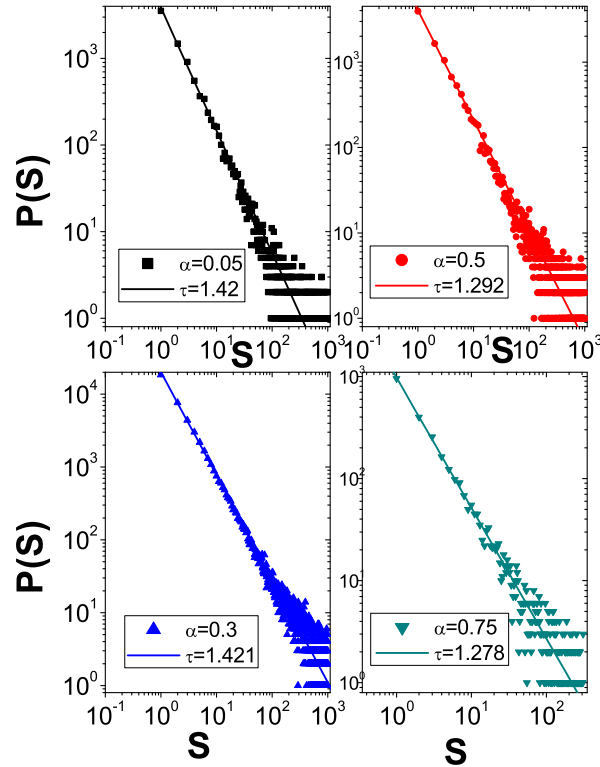


Figure 4: (color online) The probability distribution  $P(S)$  of  $\langle f \rangle_0$  avalanche as a function of the size  $S$  for one configuration of the ensemble of BSM's evolution on SFNs with various parameters  $\alpha = 0.05, 0.3, 0.5$  and  $0.75$ . The network parameters are as in Fig. 1.

where  $\tau$  is the exponent of the  $\langle f \rangle_0$  avalanche size distribution that is related to the complex system structure. The behavior of the  $\langle f \rangle_0$  avalanches differs from that of the  $f_0$  avalanches in [13], where for  $2 < \gamma < 3$ , a double power law distribution was found. The main reason is that there exists a large fluctuation of  $f$  in [13] and our definition of  $\langle f \rangle$  reduces the fluctuation in the temporal avalanches. The smaller avalanches with the size  $s < 100$  emerge with the larger probability and the larger avalanches emerge with smaller probability in [13]. Hence, the double power law distribution of  $f_0$  avalanche was found in [13] and the  $\langle f \rangle_0$  avalanche has the power law distribution in our present work. So that, our present work can show the scaling property of evolutionary dynamics of BSM better and describe the general role of complex network structure in the evolutionary dynamics of BSM, just as the complex network structure plays an important role in the epidemics dynamics in [19]. Hence, we focus on the relation between the exponent  $\tau$  and the parameter  $\alpha$ . Namely, the effects of SFN's topology on the probability distribution of  $\langle f \rangle_0$  avalanche.

In Fig. 5 we represent the evolution of  $\tau$  as a function of  $\alpha$  on SFNs with size  $N = 1000$ . We find that the  $\tau$ s of  $\langle f \rangle_0$  avalanche on SFNs are smaller than that on  $d$ -dimensional

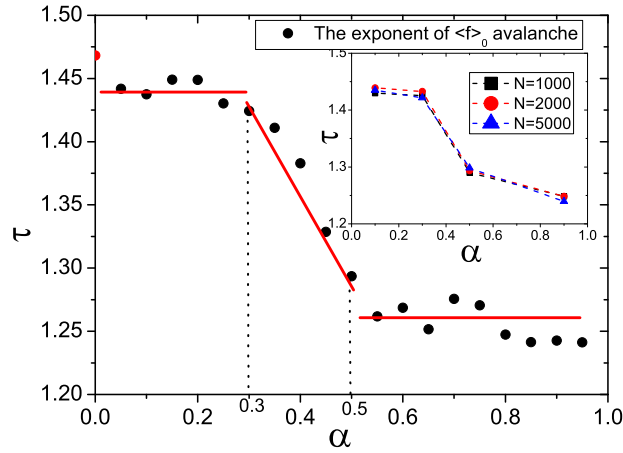


Figure 5: (color online) The evolution of the exponent  $\tau$  of  $\langle f \rangle_0$  avalanche as a function of  $\alpha$  on SFNs with size  $N=1000$ . The red dot shows the critical average fitness  $\langle f \rangle_*(\alpha)$  when  $\alpha=0$  (random network or SFN with  $\gamma=\infty$ ) and the red lines are guides to the eye. Inset: The evolution of the exponent  $\tau$  of  $\langle f \rangle_0$  avalanche as a function of  $\alpha$  on SFNs with various size  $N$ . The dashed lines are guides to the eye.

lattice [3] and on random network ( $\alpha=0$ ), which is due to the heterogeneous property of SFNs. In SFN, there exists some nodes with higher connectivity that play the same role as hubs in the internet. The higher the specie's connectivity is, the shorter the periods of intensive activity [12] will be. Interestingly, there exist the two critical values (0.3,0.5) during the evolution of the exponent  $\tau$  as a function of  $\alpha$ . For  $0.3 < \alpha < 0.5$  ( $3 < \gamma < 4.3$ ),  $\tau$  decreases as a nearly linear function of  $\alpha$ ; while, for  $0 \leq \alpha < 0.3$  ( $\gamma > 4.3$ ) and  $0.5 \leq \alpha < 1$  ( $2 < \gamma \leq 3$ ),  $\tau$ s are nearly independent of the  $\alpha$  and take 1.45(2) and 1.25(3), respectively. Furthermore, we analyze the evolution of  $\tau$  as a function of  $\alpha$  on SFNs with various size  $N$ , and find that  $\tau(\alpha)$  is independent of  $N$ , see the inset in Fig. 5. Here, we classify the SFNs into three categories: the random one for  $0 \leq \alpha < 0.3$  ( $\gamma > 4.3$ ), where the evolutionary dynamics of BSM and the epidemics dynamics [19] have the same properties as the one that occurs on random networks; the second is the linear one for  $0.3 < \alpha < 0.5$  ( $3 < \gamma < 4.3$ ), where the evolution of  $\langle f \rangle_*$  and  $\tau$  are linear decreasing functions of  $\alpha$ ; The third is the physical one for  $0.5 \leq \alpha < 1$  ( $2 < \gamma \leq 3$ ), where the evolution dynamics of BSM and the epidemics dynamics [19] share qualitatively the same results. As we know, the SFNs with the degree exponent  $2 < \gamma \leq 3$  are physical meaningful and the nodes with higher connectivity play the same role as hubs in internet. Hence, we also call the physical class as the scaling one.

To test the universality property of the scaling of  $\langle f \rangle_0$  avalanche, we analyze the evolutionary dynamics of BSM on an artificially man-made star network shown in Fig. 6. In the star network, there exists a biggest hub that connects other nodes, which do not connect each other in Fig. 6(a). We analyze the evolution of average fitness  $\langle f \rangle$  and the gap  $F(s)$  as a function of  $s$ , and find that there also exists a punctuated equilibrium, see Fig. 6(c). More interestingly, there exists a cumulative process before a huge avalanche,



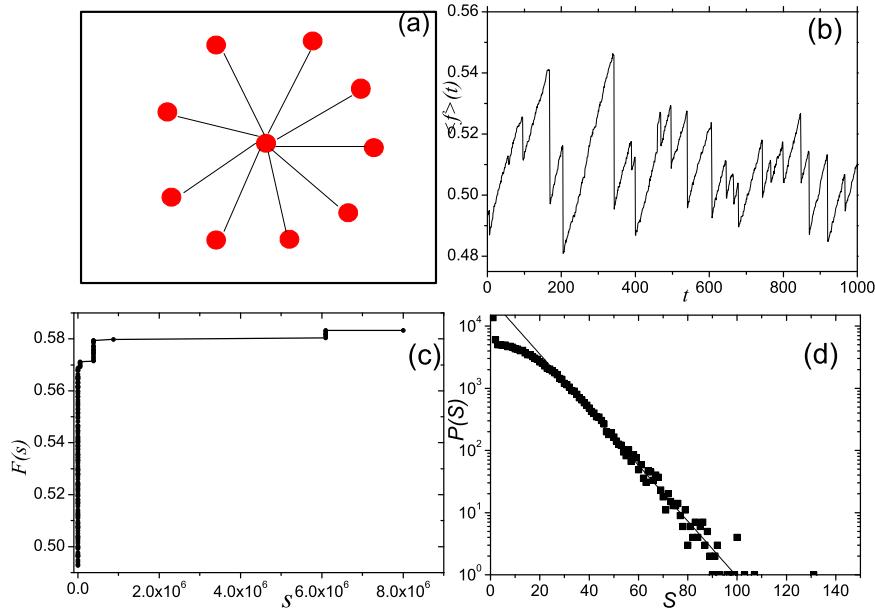


Figure 6: (color online). The evolution of (b): the average fitness  $\langle f \rangle$  as a function of time  $t$  and (c): the gap  $F(s)$  as a function of  $s$  on the man-made star network, which is constructed as (a). (d): the probability distribution  $P(S)$  of  $\langle f \rangle_0$  avalanche as a function of size  $S$ . The size of the star network  $N=1000$ .

i.e., the fitness of the hub is the smallest one and all neighbors' fitness are reset again, which is confirmed by the large decreases in Fig. 6(b). On the other hand, we study the probability distribution of  $\langle f \rangle_0$  avalanche in Fig. 6(d), and find that  $P(S)$  nicely satisfies an exponentially decreasing function, which is different from that in the complex network with  $\gamma > 2$ . Namely, the scaling property of  $\langle f \rangle_0$  avalanche is lost for star networks.

## 4 Conclusions

In summary, we study the effects of complex biosystem topology on the evolutionary dynamics of BSM. We find that the average fitness  $\langle f \rangle$  and the critical average fitness  $\langle f \rangle_*$  tend to increase stepwisely and the punctuated equilibrium also emerges on SFNs. Further, we analyze the relation between  $\langle f \rangle_*$  and  $\alpha$ , and the relation between the exponent  $\tau$  of  $\langle f \rangle_0$  avalanche size distribution and  $\alpha$ , and find some interesting results that show the dependence of the evolutionary dynamics on SFNs' topology. According to the evolutionary dynamics of BSM and the epidemics dynamics [19] on SFNs, we classify the SFNs into three categories: the random one for  $\gamma > 4.3$ , the linear one for  $3 < \gamma < 4.3$  and the physical one for  $2 < \gamma \leq 3$ . Our present work provides a new perspective to understand the role of complex system topology in the evolutionary dynamics of BSM and tools to classify the complex system from the viewpoint of dynamics.

## Acknowledgments

L. Guo thanks Prof. W. Li for his valuable suggestions and comments. This work was supported by the NSFC (10635020), the programme of Introducing Talents of Discipline to Universities under Grant No. B08033, the State Key Development Program of Basic Research of China (2008CB317103) and the Key Project of Chinese Ministry of Education (306022 and IRT0624).

## References

- [1] P. Bak and K. Sneppen, *Phys. Rev. Lett.* 71 (1993) 4083.
- [2] W. Li and X. Cai, *Phys. Rev. E* 61 (2000) 5630.
- [3] W. Li and X. Cai, *Phys. Rev. E* 61 (2000) 771.
- [4] R. J. Williams and N. D. Martinez, *Nature* 404 (2000) 180.
- [5] J. Camacho, R. Guimerà and L. A. N. Amaral, *Phys. Rev. E* 65 (2002) 030901(R).
- [6] H. Jeong, B. Tombor, R. Albert, Z. N. Oltvai and A. -L. Barabási, *Nature* 407 (2000) 651.
- [7] E. Ravasz, A. L. Somera, D. A. Mongru, Z. N. Oltvai and A. -L. Barabási, *Science* 297 (2002) 1551.
- [8] S. Maslov and K. Sneppen, *Science* 296 (2002) 910.
- [9] H. Jeong, S. Mason, A. -L. Barabási, and Z. N. Oltvai, *Nature* 411 (2001) 41.
- [10] K. Christensen, R. Donangelo, B. Koiller and K. Sneppen, *Phys. Rev. Lett.* 81 (1998) 2380.
- [11] R. V. Kulkarni, E. Almaas and D. Stroud, *cond-mat/9905066*.
- [12] Y. Moreno and A. Vazquez, *Europhys. Lett.* 57 (2002) 765.
- [13] S. Lee and Y. Kim, *Phys. Rev. E* 71 (2005) 057102.
- [14] R. Albert and A. -L. Barabási, *Rev. Mod. Phys.* 74 (2002) 47.
- [15] K. -I. Goh, B. Kahng and D. Kim, *Phys. Rev. Lett.* 87 (2001) 278701.
- [16] A. -L. Barabási and R. Albert, *Science* 286 (1999) 509.
- [17] M. Paczuski, S. Maslov and P. Bak, *Phys. Rev. E* 53 (1996) 414.
- [18] W. Li and X. Cai, *Phys. Rev. E* 62 (2000) 7743.
- [19] R. Pastor-Satorras and A. Vespignani, *Phys. Rev. Lett.* 86 (2001) 3200.